Quaternary Science Reviews 185 (2018) 113–121

Contents lists available at ScienceDirect

Quaternary Science Reviews

journal homepage: www.elsevier.com/locate/quascirev

On the differences between Last Glacial Maximum and Mid-Holocene climates in southern South America simulated by PMIP3 models

Ana Laura Berman [a], Gabriel E. Silvestri [a, *], Marcela S. Tonello [b]

[a] Centro de Investigaciones del Mar y la Atmósfera/CONICET-UBA, UMI IFAECI/CNRS, Guiraldes 2160, Ciudad Universitaria, Buenos Aires, Argentina
[b] Laboratorio de Paleoecología y Palinología/Ecología y Paleoecología de Ambientes Acuáticos Continentales, Instituto de Investigaciones Marinas y Costeras (IIMyC), CONICET-UNMdP, J.B.Justo 2550, Mar del Plata, Argentina

ARTICLE INFO

Article history:
Received 13 June 2017
Received in revised form
16 December 2017
Accepted 4 February 2018

Keywords:
Last Glacial Maximum
Mid-Holocene
South America
Pampa
Patagonia
PMIP3 models

ABSTRACT

Differences between climate conditions during the Last Glacial Maximum (LGM) and the Mid-Holocene (MH) in southern South America inferred from the state-of-the-art PMIP3 paleoclimatic simulations are described for the first time in this paper. The aim is to expose characteristics of past climate changes occurred without human influence. In this context, numerical simulations are an indispensable tool for inferring changes in near-surface air temperature and precipitation in regions where proxy information is scarce or absent. The analyzed PMIP3 models describe MH temperatures significantly warmer than those of LGM with magnitudes of change depending on the season and the specific geographic region. In addition, models indicate that seasonal mean precipitation during MH increased with respect to LGM values in wide southern continental areas to the east of the Andes Cordillera whereas seasonal precipitation developed in areas to the west of Patagonian Andes reduced from LGM to MH.

1. Introduction

The evolution of global climate during the last 21,000 years synthesizes the effects of changes in atmospheric greenhouse gas concentrations, aerosols, ice sheets, sea level, vegetation and Earth's orbital parameters. Terrestrial and marine paleorecords contain essential information regarding climate changes but model simulations are a valuable tool to reconstruct past conditions in areas where proxy information is scarce or absent. In this context, global and regional characteristics of the Last Glacial Maximum (LGM, ~21,000 yr BP) and the Mid-Holocene (MH, ~6000 yr BP) climates were analyzed considering different model simulations (e.g., Wainer et al., 2005; Otto-Bliesner et al., 2006; Melo and Marengo, 2008; Kim et al., 2008; Rojas et al., 2009; Rojas and Moreno, 2011; Kageyama et al., 2013; Chevalier et al., 2017). In South America, the study of Prado et al. (2013a) was the first description of differences between MH and modern climates considering both multiproxy paleodata compilation and model simulations included in the Paleoclimate Modeling Intercomparison Project Phase III (PMIP3). Using the same concept, the studies of Berman et al. (2016, 2017) combined information from proxies and PMIP3 simulations in order to provide a complete picture of LGM and MH climates in the southern portion of the continent as well as the corresponding differences with respect to present-day conditions. Although these previous studies constitute a significant progress in descriptions of LGM and MH climates in areas of South America, there is still a lack of analyses focused on the differences between both past periods (i.e., the study of how different MH climate conditions were with respect to those of LGM). Assessing these differences would improve the knowledge of time evolution of the climate system in the past and provide significant information about climate changes occurred without human influence. This type of analysis is crucial since it can lead to improvements of future scenarios associated with interactions between natural and anthropogenic forcings. In consequence, the aim of this paper is to explore for the first time how southern South American near-surface air temperature and precipitation changed from LGM to MH according to the state-of-the-art PMIP3 global models. Due to the availability of model outputs, the study is

* Corresponding author. Centro de Investigaciones del Mar y la Atmosfera (CIMA/CONICET-UBA), Instituto Franco-Argentino para el Estudio del Clima y sus Impactos (UMI IFAECI/CNRS-CONICET-UBA), Intendente Güiraldes 2160, Ciudad Universitaria, Buenos Aires, Argentina.
E-mail addresses: alberman@cima.fcen.uba.ar (A.L. Berman), gabriels@cima.fcen.uba.ar (G.E. Silvestri), mtonello@mdp.edu.ar (M.S. Tonello).

https://doi.org/10.1016/j.quascirev.2018.02.003
0277-3791/

focused on differences between the specific time windows defined as LGM and MH for the PMIP3 experiments (see details in Section 2) omitting descriptions of climate changes occurred during the lateglacial and early Holocene.

The manuscript is organized as follows: data and methodology are described in section 2, differences between LGM and MH temperature and precipitation are analyzed in section 3 and the main conclusions are summarized in section 4.

2. Data and methodology

2.1. Data

2.1.1. Paleoclimate proxies

A suite of paleoclimate proxies reflecting local changes in temperature and/or precipitation over the portion of South America to the south of 20°S constitutes the primary picture to contrast LGM and MH climates and it is also a valuable tool to test the quality of PMIP3 models. In this paper, LGM and MH represent two key time windows: LGM encompass the interval 18,000–24,000 cal yr BP (centered at ~21,000 cal yr BP) whereas MH comprises the interval 5000–7000 cal yr BP (centered at ~6000 cal yr BP). Both intervals are adopted in order to be consistent with the time windows simulated in the PMIP3 experiments (see Section 2.1.2).

Several studies reconstructed characteristics of temperature and precipitation in sites of southern South America during glacial and post-glacial times. However, only few of them describe how different the LGM mean conditions were with respect to those of the MH considering LGM and MH as the time windows indicated in the previous paragraph. After a bibliographic review, we found only eight references of sites in the study area with paleoclimatic information providing clear descriptions of differences between LGM and MH climate conditions to be contrasted against outputs of PMIP3 experiments. The criterion to select the sites involves two specific conditions: (1) records have to present a continuous sedimentation and the periods LGM and MH have to be represented; and (2) dating controls have to include at least one data within the range of the corresponding time window (i.e., 18,000–24,000 cal yr BP for LGM and 5000–7000 cal yr BP for MH). This criterion implies not only the definition of a specific time window for each past period but also that both periods have to be included in the same record to be consistent with the information provided by each grid point of each PMIP3 model.

The selection of sites with paleoclimate information is a crucial step in model-data comparison. Although several paleoclimate proxies describe LGM and MH climates with useful information to validate PMIP3 simulations (e.g., Wainer et al., 2005; Prado et al., 2013b; Berman et al., 2016, 2017), the list of sites satisfying the above-mentioned criterion reduces to that exhibited in Fig. 1 (the corresponding climate changes are summarized in Section 3).

2.1.2. Model simulations

This study considers simulations of LGM and MH climates using coupled ocean-atmosphere general circulation models carried out under the PMIP3 framework. In both paleoclimatic experiments, models were run with very specific boundary conditions that include, among others, specifications for insolation, atmospheric composition, orography, land-sea geography, surface type, ice sheet, vegetation, carbon cycle and ocean salinity. The imposed boundary conditions in the PMIP3 experiments of LGM are conditions inferred for 21,000 yr BP while those of MH correspond to 6000 yr BP. The most conspicuous differences between the boundary conditions for LGM and MH simulations are: i) Reduced LGM concentration in atmospheric greenhouse gases relative to MH values; ii) Significant expansion of ice sheets in the Northern Hemisphere during LGM; iii) Decreased (increased) LGM insolation over the Southern (Northern) Hemisphere in winter-spring and increased (decreased) in summer-autumn compared to MH conditions due to changes in orbital parameters of the Earth around the Sun. Detailed description of these experiments can be found in Braconnot et al. (2012) and Taylor et al. (2012).

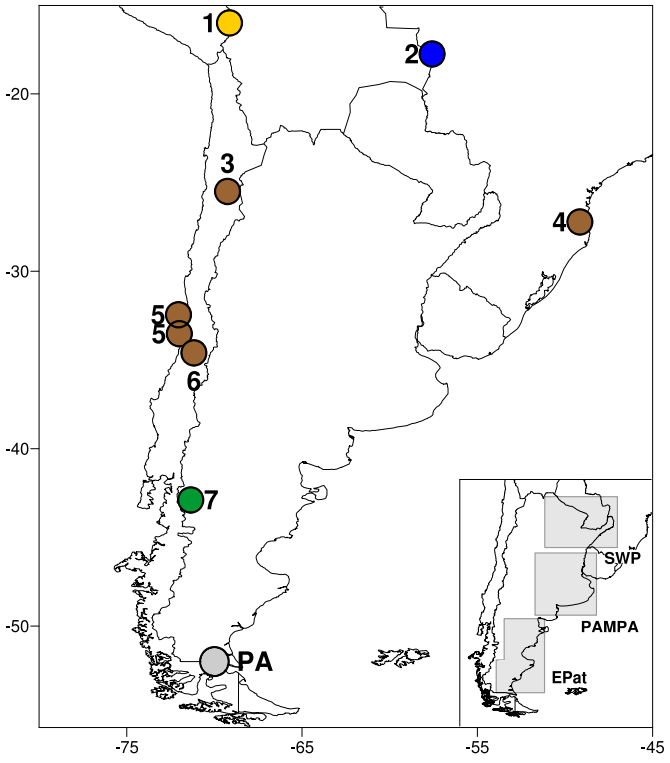

Fig. 1. Paleoclimate proxy data compilation for differences between MH and LGM climates. Orange point (●) indicates MH warmer and drier than LGM. Blue point (●) indicates MH warmer and wetter than LGM. Brown points (●) indicate MH drier than LGM. Green point (●) indicates MH wetter than LGM. Gray point (●) indicates the Lake Potrok Aike (PA). See the corresponding references in Section 3.1. Shaded continental areas in the map of the right-bottom corner indicate the sub-regions Subtropical Wet Plain (SWP), Pampa and Eastern Patagonia (EPat) mentioned throughout the text. (For interpretation of the references to colour in this figure legend, the reader is referred to the Web version of this article.)

Four models were selected for the study: CCSM4, CNRM-CM5, MPI-ES-P and MRI-CGCM3 (see Table 1). Focusing on southern South America, these models have the ability to reproduce the paleoclimate proxy reconstructions of changes between LGM and present (Berman et al., 2016) and between MH and present (Berman et al., 2017). In addition, the four selected models reproduce the main features of changes between LGM and MH inferred from sites available in the region (see Section 3). Although there are other four models describing LGM and MH climates in the PMIP3 database, they were excluded from this analysis due to one of the following reasons: i) Erroneous representation of climate changes inferred from regional proxies; ii) Low spatial resolution (high density of grid points is important to describe the influence of the Andes Cordillera on regional precipitation); iii) Deficiencies in representing spatial fields of seasonal mean precipitation in tropical-subtropical areas of South America.

2.2. Methodology

The analysis is focused on changes of near-surface air temperature and precipitation over the portion of South America to the south of 20°S comprising Argentina, Chile, Paraguay, Uruguay,

Table 1
PMIP3 models employed in the study.

Model name	Institution	Atmosphere resolution (lon x lat)	Reference(s)
CCSM4	National Centre for Atmospheric Research (USA)	1.25° x ~0.9°	Gent et al. (2011)
CNRM-CM5	Centre National de Recherches Météorologiques, Centre Européen de Recherche et de Formation Avancée en Calcul Scientifique (France)	~1.4° x ~1.4°	Voldoire et al. (2012)
MPI-ESM-P	Max Planck Institute for Meteorology (Germany)	~1.8° x ~1.8°	Jungclaus et al. (2012a; 2012b)
MRI-CGCM3	Meteorological Research Institute (Japan)	~1.12° x ~1.12°	Yukimoto et al. (2012)

southern Bolivia and southern Brazil. As detailed in Berman et al. (2016), three sub-regions are specially considered throughout the analysis to synthesize climate changes in the area to the east of the Andes Cordillera (see inset in Fig. 1): the subtropical wet plain (SWP), the temperate Pampa and the arid eastern Patagonia (EPat).

Seasonal mean conditions are analyzed considering austral summer as December-January-February (DJF), autumn as March-April-May (MAM), winter as June-July-August (JJA) and spring as September-October-November (SON). Statistics correspond to simulations of 100 years of both LGM and MH. The Student's t-test (Wilks, 2006) is applied to assess the statistical significance of differences between the past periods (i.e., differences MH minus LGM).

3. Results and discussion

3.1. Paleoclimate proxies synthesis

Table 2 compiles the selected sites and Fig. 1 shows the corresponding change in temperature and/or precipitation from LGM to MH. Without explicit indications about seasonal changes in the corresponding bibliographic reference, it is assumed that inferences correspond to annual mean conditions. Information from each site can be synthesized as follows:

1) Pollen and charcoal analyses from Lake Titicaca (site 1) suggest MH temperatures higher than those registered during glacial times (Paduano et al., 2003). Hydrogen isotopic composition analysis of sediment cores at the same site indicates drier conditions during the Holocene relative to LGM (Fornace et al., 2014). Authors proposed that this change might have corresponded to summer conditions because most of regional precipitation falls during that season.
2) A multiproxy analysis on sediment records from Lake La Gaiba (site 2) provides evidence that the climate was markedly warmer and wetter during MH compared to LGM mean conditions (Whitney et al., 2011).
3) Pollen evidence from Quebrada del Chaco (site 3) indicates reduced winter precipitation during MH with respect to glacial mean values (Maldonado et al., 2005). This site does not fulfill the criterion 1 of section 2.1.1 due to fossil rodent middens are stratigraphically discontinuous. However, it was included in the analysis because middens become the primary source of paleoclimate information about late Quaternary in the Atacama desert.
4) A speleothem record from Caverna Botuverá (site 4) suggests that MH precipitation was lower than that registered during LGM (Wang et al., 2007). Authors proposed that increased moisture advection from the Amazon during glacial summers might have produced this change.
5) Marine sediment cores from the continental slope off mid-latitude Chile (sites 5) indicate that glacial climates were generally humid while a trend toward arid conditions prevailed during MH (Lamy et al., 1999). These inferences suggest reduction of precipitation from LGM to MH.
6) A multiproxy record of past vegetation and hydrological changes in Laguna de Tagua Tagua (site 6) shows humid LGM climate and extremely arid conditions during MH (Valero-Garcés et al., 2005). In consequence, precipitation might have reduced during MH compared to glacial values.
7) Pollen and charcoal data from Laguna La Zeta together eleven sites located along the eastern flanks of Patagonian Andes (41–43°S, site 7) indicate that since the Lateglacial climate became progressively wetter (Iglesias et al., 2014). This result suggests that precipitation over that specific area might have increased from LGM to MH.

As it was previously mentioned, the study is focused on the portion of South America to the south of 20°S. Consequently, sites 1 and 2 are outside this region (both sites are located at ~16-17°S). However, information from these sites is included in the analysis due to the scarcity of paleorecords in the selected area (sites 1 and 2 provide the unique reference of temperature changes from LGM to MH in the south of South America). On the other hand, multiproxy reconstruction of lake-level history of Lake Potrok Aike located in southernmost Patagonia (see Fig. 1) indicates that the level during LGM was higher than during MH (Zolitschka et al., 2013). Nevertheless, this information has to be considered with caution because the level of this lake might have been controlled by multiple factors (e.g., snowmelt, evaporation, surface-subsurface runoff) without

Table 2
Site name, analyzed proxy, reconstructed variable, chronological control (number of dating in the intervals corresponding to LGM and MH) and reference. See Fig. 1 for sites locations.

Site N°	Site name	Proxy	Reconstructed variable	Chronological control		Reference
				LGM	MH	
1	Lake Titicaca	pollen and charcoal	temperature	4	3	Paduano et al. (2003)
		isotope	precipitation	1	1	Fornace et al. (2014)
2	Lake La Gaiba	multiproxy analysis	temperature	3	2	Whitney et al. (2011)
3	Quebrada del Chaco	pollen	precipitation	4	2	Maldonado et al. (2005)
4	Caverna Botuverá	speleothem	precipitation	1	1	Wang et al. (2007)
5	mid-latitude Chile	marine sediment	precipitation	5	2	Lamy et al. (1999)
6	Laguna de Tagua Tagua	multiproxy analysis	precipitation	2	1	Valero-Garcés et al. (2005)
7	Patagonian Andes	pollen and charcoal	precipitation	1	2	Iglesias et al. (2014)

clear influence of changes in only one climatic variable as local temperature or precipitation.

3.2. Model simulations

In light of the data compilation summarized in Fig. 1, there is a lack of sites in wide areas of southern South America providing suitable information of climate changes between the time windows here considered as LGM and MH. Consequently, simulations carried out with PMIP3 models constitute an indispensable tool to describe changes of near-surface air temperature and precipitation over the region.

3.2.1. Temperature

Simulated spatial fields of near-surface air temperature over South America during LGM and MH show the same two main features observed in the present climate (see Supplementary Fig. S1): i) A north-south gradient due to the reduction of insolation from equatorial to higher latitudes; ii) Marked annual cycles with warm summers and cold winters in response to the annual cycle of insolation. Although the spatial structure of seasonal mean fields and the annual cycles during LGM were qualitatively similar to those of MH, the four models show significant differences between the corresponding seasonal mean values in the entire continent. These differences are shown in Fig. 2. Specific characteristics in sub-regions SWP, Pampa and EPat are detailed in Fig. 3. The most relevant aspects of temperature changes displayed by these figures can be synthesized as follows.

The four models show MH annual mean temperature significantly higher than that of LGM in the entire South America but there are inter-model differences in the magnitude of simulated changes (Fig. 2). Models exhibit a MH warming of ~2–4 °C over most of the continent and the sign of the change agree with local conditions proposed by paleoclimate proxies in sites 1 and 2 (see Fig. 1). Significant MH warming is also simulated over the oceans except in small areas of the Southwestern Atlantic in models CNRM and MPI where changes of temperature were affected by changes in sea level (see more details in the following paragraphs).

Simulations of summer conditions display generalized significant MH warming over South America with inter-model differences in the corresponding magnitudes (Fig. 2). In the southern subregions, models suggest MH warming of ~1.6–3.1 °C in SWP, ~0.7–2.9 °C in Pampa and ~0.3–2.6 °C in EPat (Fig. 3). It is important to take into account that the Argentine Continental Shelf was exposed during LGM due to the global fall of sea levels (e.g., Rostami et al., 2000; Ponce et al., 2011). Models represent this sea-level change in the South American coast and suggest that summer temperature over those glacial lands was ~4–6 °C warmer than temperature over the cold sea waters that covered the region in MH. The effect of summer insolation heating the exposed glacial lands can explain this change of temperature.

Significant and generalized MH warming over South America persists during autumn with magnitudes of ~1–4 °C depending on the model and the region (Fig. 2). Models suggest MH warming of ~1.4–3.3 °C in SWP, ~1.3–3.7 °C in Pampa and ~1.2–3.3 °C in EPat (Fig. 3). Glacial heating over the Argentine Continental Shelf was reduced or absent during this season due to weakened insolation as consequence of the annual cycle of incoming solar radiation in middle latitudes.

Modeled winter temperatures during MH are ~2–4 °C warmer than those of LGM over most of South America but a more pronounced warming of ~4–6 °C is simulated over the southern tip of the continent by the four models (Fig. 2). A detailed inspection of the specific seasonal values modeled in the southernmost continental areas reveals that LGM temperatures were lower than 0 °C in almost all glacial winters but only few years repeat the same condition during MH. In the selected sub-regions, models suggest differences of ~2.3–4.2 °C in SWP, ~1.5–3.9 °C in Pampa and ~3.5–4.7 °C in EPat (Fig. 3). The annual cycle of incoming solar radiation has minimum values during this season reducing the solar heating of exposed glacial lands in the Argentine Continental Shelf. This feature can explain that glacial superficial temperatures were colder than those of the ocean waters that covered the region in MH.

Simulated changes of temperature during spring suggest MH warming of ~4–7 °C over wide tropical-subtropical continental areas (Fig. 2) and differences of ~3.1–4.5 °C in SWP, ~2.4–4.3 °C in Pampa and ~2.0–5.3 °C in EPat (Fig. 3). In contrast, increased insolation in middle latitudes due to the natural annual cycle restored warmer glacial conditions over the exposed lands in the Argentine Continental Shelf.

Climate transition from LGM to MH in South America was partially influenced by changes in orbital parameters of the Earth around the Sun that, in turn, modified the incoming solar radiation at the top of the atmosphere and the Earth's radiative balance. In fact, South America is located in latitudes where solar radiation during MH reduced in summer-autumn and increased in winter-spring with respect to the conditions during the glacial period (see Section 2.1.2 and Fig. 1 in Otto-Bliesner et al., 2006). These insolation changes explain that magnitudes of MH warming described by the numerical simulations over continental areas are lower in summer-autumn and higher in winter-spring (see Fig. 2).

3.2.2. Precipitation

Spatial patterns of seasonal precipitation over South America during LGM and MH exhibit three conspicuous features qualitatively similar to those of the present climate (see Supplementary Fig. S2):

i) Precipitation over wide tropical-subtropical areas has a marked annual cycle with rainy summers and dry winters. During summer, an elongated band of intense convection and precipitation, named South Atlantic convergence zone (SACZ) (e.g., Carvalho et al., 2004), extends from the Amazon basin to the subtropical Atlantic Ocean. Reduced insolation in autumn-winter reduces the intensity of the SACZ and convective systems producing abundant precipitation migrate to the northern tip of the continent. During spring, insolation gradually increases and the SACZ is restored achieving its maximum intensity with the beginning of the new summer.

ii) Precipitation over broad subtropical areas comprising northern and central Argentina is closely connected with moisture advection from the Amazon and from the subtropical Atlantic Ocean. This advection is more intense in summer than in winter and, consequently, precipitation over that subtropical portion of the continent has an annual cycle with rainy summers and dry winters.

iii) Precipitation over Patagonia, the region to the south of 40°S, is mainly produced by migratory low-level systems moving to the east along the Southern Hemisphere storm tracks. The Andes Cordillera is an orographic obstacle for the air masses arriving from the Pacific Ocean enhancing the synoptic-scale precipitation over the mountains and adjacent areas. In consequence, a significant climatic contrast is generated over this region with hyper-humid conditions around the mountains and arid-semiarid ecosystems in the eastern Argentinian steppe. This feature persists through the year but maximum precipitation migrates to the north (south) in

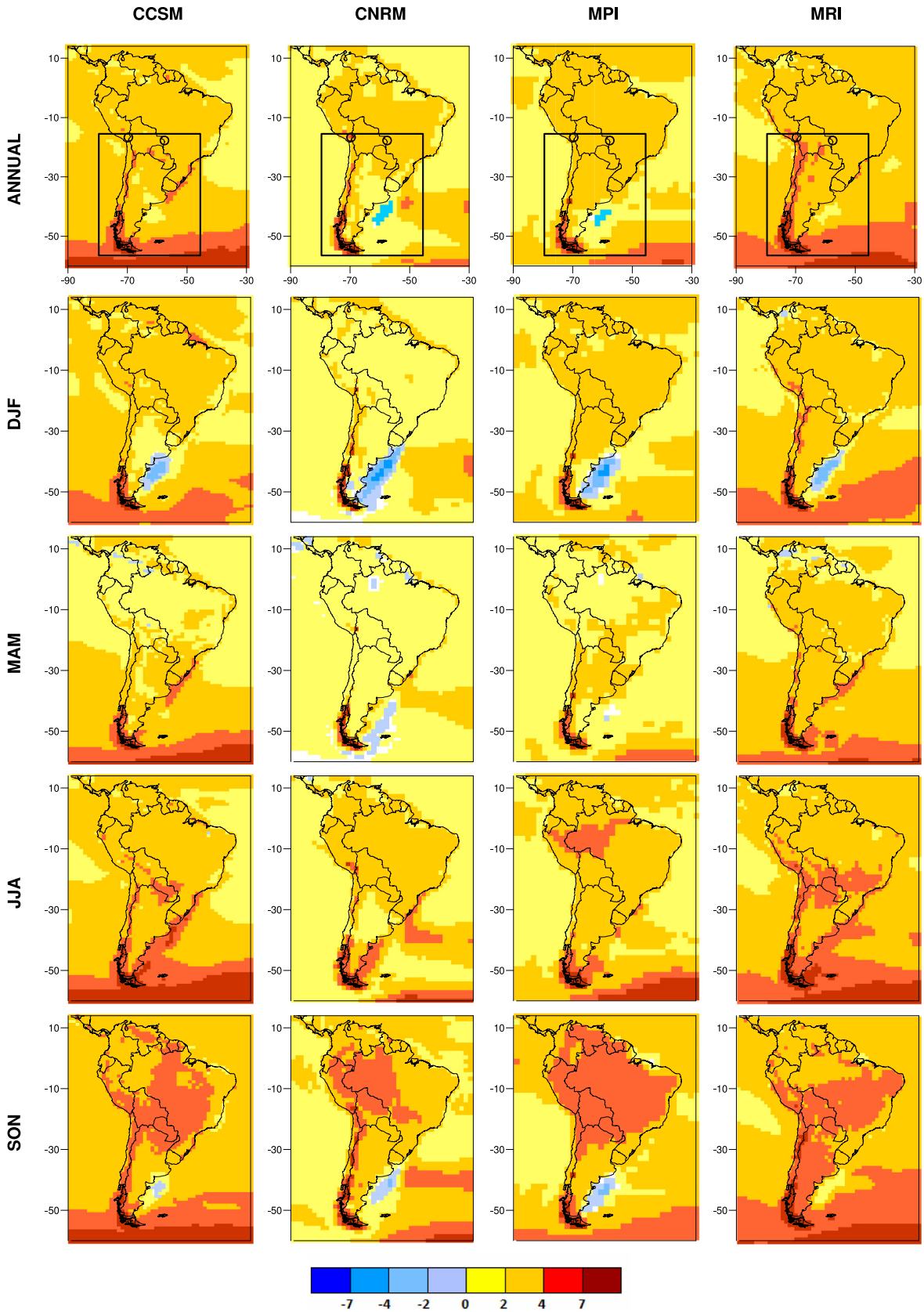

Fig. 2. Differences MH minus LGM for annual and seasonal mean near-surface air temperature simulated by each PMIP3 model. Differences are significant at 95% in all grid points except in the few ones in white. Empty circles in maps of annual differences indicate sites where MH was warmer than LGM (see Fig. 1 and Table 2). Black squares in maps of annual differences delimit the area of Fig. 1.

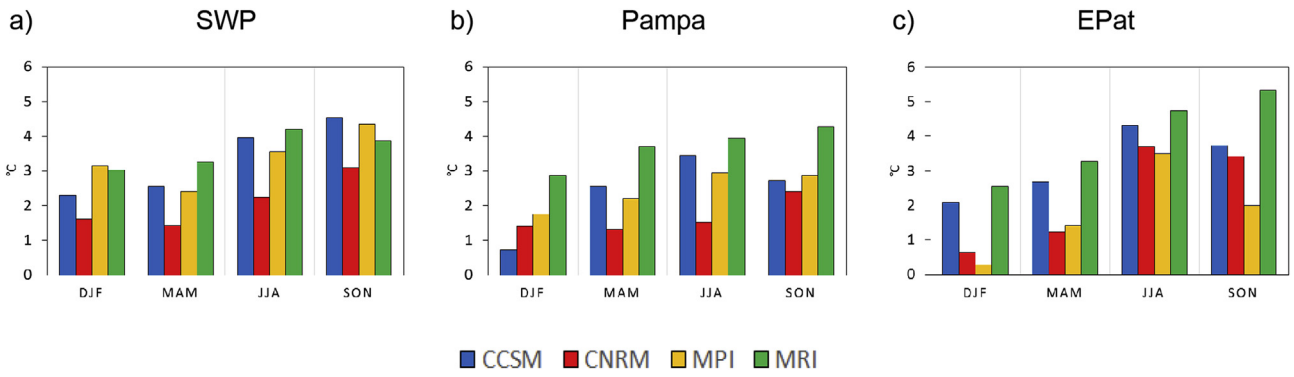

Fig. 3. Differences MH minus LGM for seasonal mean near-surface air temperature simulated by each PMIP3 model in the sub-regions SWP, Pampa and EPat.

winter (summer) following the most frequent tracks of synoptic migratory systems.

Although the spatial structure of seasonal mean fields of precipitation over the continent during LGM and MH were qualitatively similar, the four models show significant changes in the magnitude of precipitation registered in each past period. These changes are shown in Fig. 4 and specific conditions in the three southern sub-regions are highlighted in Fig. 5. The most relevant characteristics displayed by these figures can be synthesized as follows.

Differences between annual mean values reveal discrepancies among models in the sign of the change over wide continental areas to the north of ~30°S (Fig. 4) where sites 1, 2 and 4 are located (see Fig. 1). In contrast, the four models agree to simulate significant increment of annual mean precipitation during MH with respect to LGM mean values in central-southern Argentina, and reduced magnitude of the local maximum developed over southern Chile. These latter features coincide with precipitation changes inferred in sites 5, 6 and 7 (see Fig. 1).

In summer, the four models describe increased MH precipitation over the northern tip of the continent but marked disagreements are detected in the sign and magnitude of the change over continental areas in 0°–30°S including the sub-region SWP (Fig. 4). These inter-model differences might be produced by discrepancies in the representation of atmospheric water vapor content and dynamic-thermodynamic processes that dominate the development of convective precipitation in those regions. On the other hand, models disagree in the magnitude of the changes over the southern portion of the continent, but the four simulations describe increased MH precipitation over sub-regions Pampa (increment of 11–32%) and EPat (increment of 32–120%) (Fig. 5). The four models also agree in representing reduction of MH precipitation in the area of the local maximum developed around southern Chile.

Increased MH precipitation over the northern tip of the continent and inter-model differences in the sign and magnitude of the change over central Brazil persist during autumn (Fig. 4). In areas to the south of 20°S, models agree on the following conditions in this season: i) Reduced MH precipitation over Paraguay, northeastern Argentina and southern Brazil (reduction of 11–19% in SWP, Fig. 5a); ii) Increased MH precipitation over central and southern Argentina (increment of 1–17% in Pampa and 65–101% in EPat, Fig. 5b–c); iii) Reduced magnitude of the local maximum around southern Chile in MH compared to LGM mean values (Fig. 4).

In winter, the four models describe significant reduction of precipitation during MH with respect to LGM conditions over wide tropical-subtropical continental areas but there are inter-model differences in the magnitude and specific geographical distribution of this change (Fig. 4). Subtropical areas with reduced MH precipitation comprise northern Chile coinciding with the seasonal change inferred from the site 3 (see Fig. 1) and include the sub-region SWP where modeled MH values are 5–28% lower than those of glacial times (Fig. 5a). Southward, models agree to simulate increased MH precipitation over Pampa (8–35%, Fig. 5b) and EPat (76–101%, Fig. 5c) while the magnitude of the local maximum over southern Chile was reduced during MH (Fig. 4).

Simulations of spring precipitation show inter-model differences in the sign and magnitude of changes in areas to the north of 20°S (Fig. 4). On the other hand, the four models suggest increased MH precipitation over SWP (2–28%, Fig. 5a), Pampa (14–51%, Fig. 5b) and EPat (59–134%, Fig. 5c) as well as reduced magnitude of the local maximum over southern Chile during MH with respect to glacial values (Fig. 4).

In light of results here exposed, the previously mentioned reduction of the level of Lake Potrok Aike in MH with respect to LGM conditions (see Section 3.1) might be not directly connected to precipitation changes because model simulations indicate increased MH precipitation over the southernmost portion of the continent. Consequently, higher levels in this lake during glacial times might be consequence, among other possible forcings, of reduced evaporation due to lower regional temperatures as those described in Section 3.2.1.

The study of atmospheric anomalies responsible for precipitation changes over southern South America from LGM to MH is beyond the scope of this paper. That specific analysis requires detailed investigations of changes in processes that produce precipitation in each sub-region. In this context and based on present-day conditions, precipitation over sub-regions SWP and Pampa depends on appropriated moisture flow from tropical latitudes and from the subtropical Atlantic but it is also affected by frequency of passage of atmospheric fronts (e.g., Catto et al., 2012), activity of cyclonic systems originating in the cyclogenesis region of subtropical South America (e.g., Hoskins and Hodges, 2005) and the development of convective systems produced by intense surface heating (e.g., Rasmussen et al., 2016). Also based on present-day conditions, precipitation changes in Patagonia might be related to interactions between changes in characteristics of storm tracks and their associated frontal systems (e.g., Catto et al., 2012), intensity and/or position of westerly winds (e.g., Berman et al., 2012), frequency of atmospheric blocking events (e.g., Agosta et al., 2015) and local effects associated with orography of the southern Andes (e.g., Garreaud et al., 2013). Further studies should investigate if the increment of precipitation over eastern Patagonia and southern oceans during MH was induced by more frequent and/or more intense migratory cyclones and frontal systems tracking in middle and high latitudes. Those companion studies should also

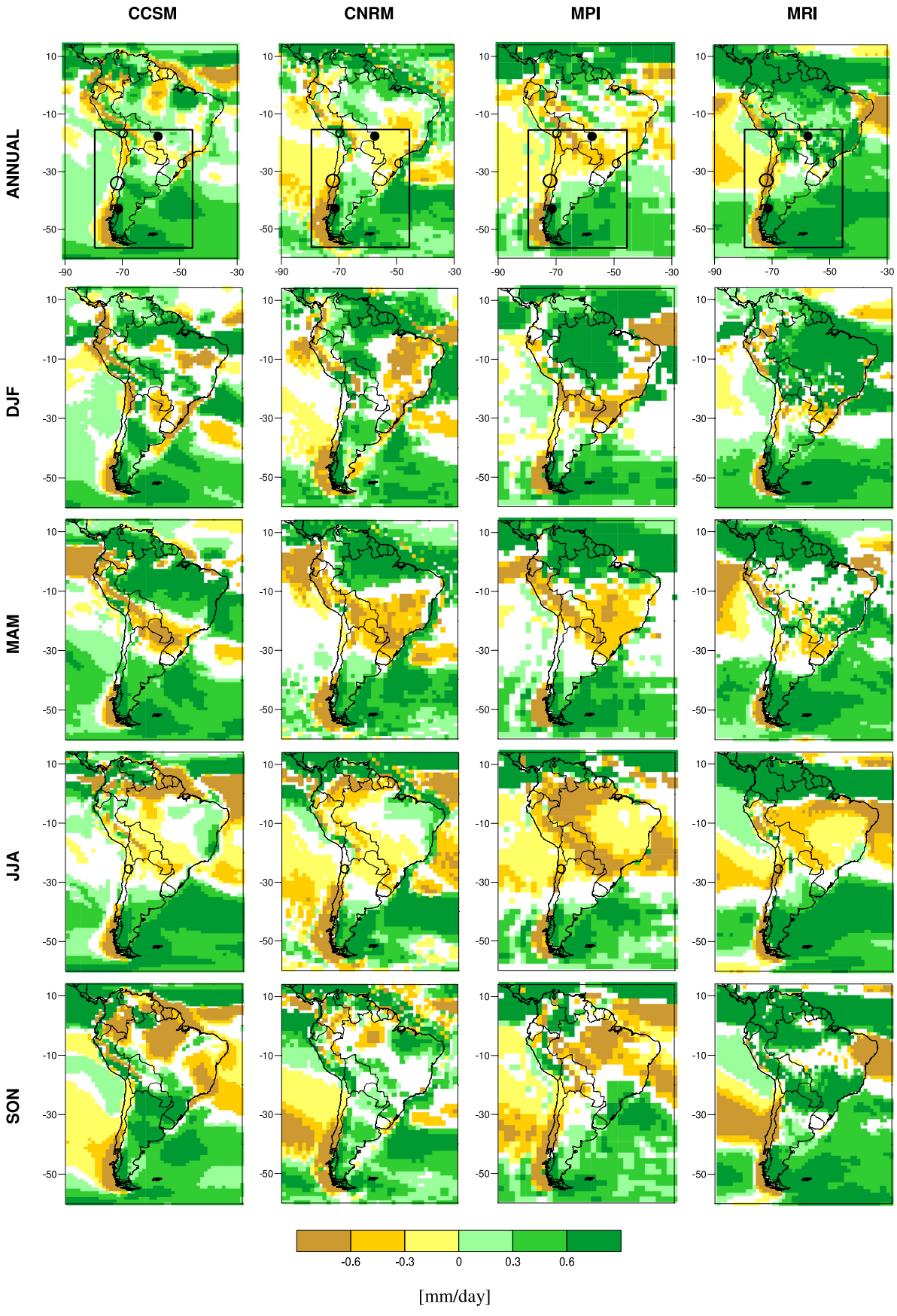

Fig. 4. Differences MH minus LGM for annual and seasonal mean precipitation simulated by each PMIP3 model. Only differences significant at 95% are shown. Empty (filled) circles in maps of annual and winter differences indicate sites where MH precipitation was lower (higher) than that of LGM (see Fig. 1 and Table 2). Due to graphical reasons, one circle of high size represents the conditions in sites 5 and 6. Black squares in maps of annual differences delimit the area of Fig. 1.

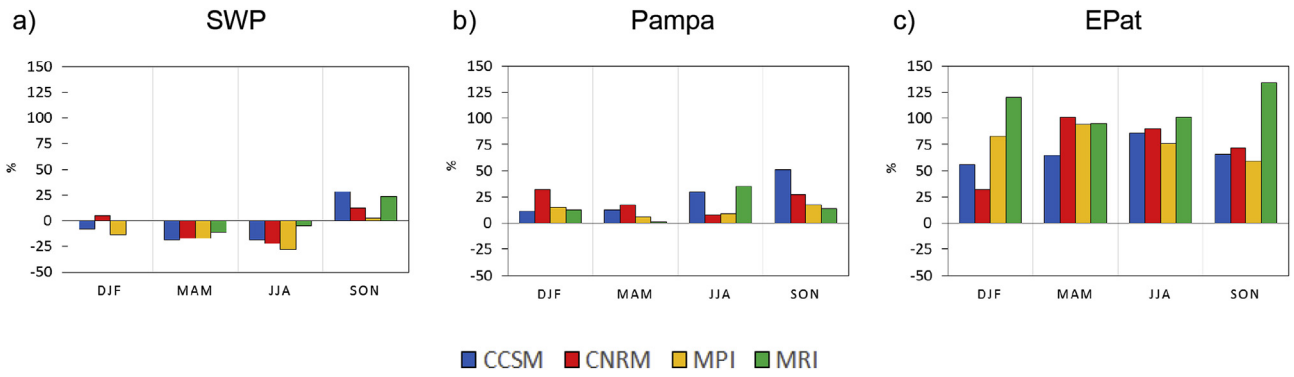

Fig. 5. Differences between MH and LGM seasonal mean precipitation (PR) simulated by each PMIP3 model in the sub-regions SWP, Pampa and EPat. Differences are percentages of MH precipitation with respect to LGM mean values: difference = [(PR_{MH} x 100/PR_{LGM}) - 100].

investigate if increased Patagonian ice sheets in glacial times (e.g., Hulton et al., 2002) intensified orographic processes inducing more precipitation on the windward side of the mountains during LGM. In other words, precipitation changes over Patagonia and the surroundings oceans displayed in Fig. 4 might be the result of a combination of changes in large-scale atmospheric conditions associated with migratory synoptic perturbations and changes in local events connected with orographic effects of the southern Andes.

4. Conclusions

This study shows, for the first time, differences between LGM and MH climates in southern South America described by coupled ocean-atmosphere general circulation models included of the suite of PMIP3 paleo-experiments. The analysis explores changes in annual and seasonal mean conditions of near-surface air temperature and precipitation over the entire continent with especial focus on the area to the south of 20°S comprising wet-temperate plains and the arid eastern Patagonia. Results displayed in this paper constitute an innovative contribution to the knowledge of past climate changes occurred in the region. Although model outputs do not replace paleoclimate proxies, PMIP3 numerical simulations are an indispensable tool to reconstruct changes of near-surface air temperature and precipitation between LGM and MH in areas of southern South America where proxy information is scarce or absent. In this context, models used throughout the study properly reproduce conditions inferred from the available paleoclimate proxy data. Consequently, these models provide reliable information about past climate changes in the region.

The analyzed simulations suggest that annual and seasonal mean temperatures during MH were significantly warmer than those of LGM over the entire South America. This warming was more pronounced during winter and spring coinciding with seasons of increased MH insolation in the Southern Hemisphere due to changes in orbital parameters of the Earth around the Sun. Although all models agree on the sign of the temperature shift (i.e., warmer conditions during MH), there are marked discrepancies among them in the specific magnitude of the change. Modeled seasonal differences MH minus LGM in the southern portion of the continent are ~1–5 °C depending on the model, season and geographic region.

Regarding annual and seasonal mean precipitation, inter-model differences are detected in the sign of the change over wide tropical-subtropical areas. In contrast, models agree on the following characteristics of precipitation changes over the southern portion of the continent: i) Reduced (increased) MH precipitation in sub-region SWP in autumn and winter (spring); ii) Increased MH precipitation in sub-regions Pampa and EPat during the four seasons. Models indicate that the most pronounced precipitation change took place over eastern Patagonia where MH seasonal precipitation was 32–134% (depending on the model and season) higher than the mean values during LGM.

Further analyses must be done in order to identify changes in hemispheric and regional atmospheric circulation patterns that induced shifts of seasonal precipitation from LGM to MH over South America. Atmospheric conditions affecting the southern portion of the continent must be analyzed with extreme caution taking into account all potential perturbations connected with regional precipitation. Some questions that should be addressed in upcoming studies are: What was the change in atmospheric water vapor flow from tropical to subtropical areas?; What was the change in storm tracks, frontal activity, blocking systems and westerly winds around Patagonia?; What was the interaction between migratory synoptic systems and Patagonian ice sheets? Answering these questions will help to understand the evolution of the South American climate through time.

Acknowledgements

Ana Laura Berman and Gabriel Silvestri were financed by Grant AGENCIA-MINCYT-PICT-2013-0043. Marcela Tonello was supported by Grants UNMdP EXA807/16 and UNMdP EXA775/16. Authors acknowledge the climate modeling groups (listed in Section 2) for producing and making available their model output. Comments and suggestions provided by Vera Markgraf and an anonymous reviewer were very helpful in improving this paper.

Appendix A. Supplementary data

Supplementary data related to this article can be found at https://doi.org/10.1016/j.quascirev.2018.02.003.

References

Agosta, E., Campagnucci, R., Ariztegui, D., 2015. Precipitation linked to Atlantic moisture transport: clues to interpret Patagonian palaeoclimate. Clim. Res. 62, 219–240.
Berman, A.L., Silvestri, G., Compagnucci, R., 2012. Eastern Patagonia seasonal precipitation: influence of southern hemisphere circulation and links with subtropical South American precipitation. J. Clim. 25, 6781–6795.
Berman, A.L., Silvestri, G., Tonello, M., 2016. Differences between last glacial maximum and present-day temperature and precipitation in southern South America. Quat. Sci. Rev. 150, 221–233.
Berman, A.L., Silvestri, G., Rojas, M., Tonello, M., 2017. Accelerated greenhouse gases versus slow insolation forcing induced climate changes in southern South America since the Mid-Holocene. Clim. Dyn 48, 387–404.

Braconnot, P., Harrison, S.P., Kageyama, M., Bartlein, P.J., Masson-Delmotte, V., Abe-Ouchi, A., Otto-Bliesner, B., Zhao, Y., 2012. Evaluation of climate models using palaeoclimatic data. Nat. Clim. Change 2, 417–424. https://doi.org/10.1038/nclimate1456.

Carvalho, L., Jones, C., Liebmann, B., 2004. The South Atlantic convergence zone: intensity, form, persistence, and relationships with intraseasonal to interannual activity and extreme rainfall. J. Clim. 17, 88–108.

Catto, J.L., Jakob, C., Berry, G., Nicholls, N., 2012. Relating global precipitation to atmospheric fronts. Geophys. Res. Lett. 39, L10805. https://doi.org/10.1029/2012GL051736.

Chevalier, M., Brewer, S., Chase, B.M., 2017. Qualitative assessment of PMIP3 rainfall simulations across the eastern African monsoon domains during the mid-Holocene and the Last Glacial Maximum. Quat. Sci. Rev. 156, 107–120.

Fornace, K.L., Hughen, K.A., Shanahan, T.M., Fritz, S.C., Baker, P.A., Sylva, S.P., 2014. A 60,000-year record of hydrologic variability in the Central Andes from the hydrogen isotopic composition of leaf waxes in Lake Titicaca sediments. Earth Planet Sci. Lett. 408, 263–271.

Garreaud, R.D., Lopez, P., Minvielle, M., Rojas, M., 2013. Large scale control on the Patagonia climate. J. Clim. 26, 215–230.

Gent, P.R., Danabasoglu, G., Donner, L.J., Holland, M.M., Hunke, E.C., Jayne, S.R., Lawrence, D.M., Neale, R.B., Rasch, P.J., Vertenstein, M., Worley, P.H., Yang, Z.-L., Zhang, M., 2011. The community climate system model version 4. J. Clim. 24, 4973–4991.

Hoskins, B.J., Hodges, K.I., 2005. A new perspective on southern hemisphere storm tracks. J. Clim. 18, 4108–4129.

Hulton, N.R.J., Purves, R.S., McCulloch, R.D., Sugden, D.E., Bentley, M.J., 2002. The last glacial maximum and deglaciation in southern South America. Quat. Sci. Rev. 21, 233–241.

Iglesias, V., Whitlock, C., Markgraf, V., Bianchi, M.M., 2014. Postglacial history of the Patagonian forest/steppe ecotone (41-43°S). Quat. Sci. Rev. 94, 120–135.

Jungclaus, J., Giorgetta, M., Reick, Ch, Legutke, S., Brovkin, V., Crueger, T., Esch, M., Fieg, K., Fischer, N., Glushak, K., Gayler, V., Haak, H., Hollweg, H.-D., Kinne, S., Kornblueh, L., Matei, D., Mauritsen, T., Mikolajewicz, U., Müller, W., Notz, D., Pohlmann, T., Raddatz, T., Rast, S., Roeckner, E., Salzmann, M., Schmidt, H., Schnur, R., Segschneider, J., Six, K., Stockhause, M., Wegner, J., Widmann, H., Wieners, K.-H., Claussen, M., Marotzke, J., Stevens, B., 2012a. CMIP5 Simulations of the Max Planck Institute for Meteorology (MPI-M) Based on the MPI-ESM-P Model: the Lgm Experiment. served by ESGF. WDCC at DKRZ. https://doi.org/10.1594/WDCC/CMIP5.MXEPlg.

Jungclaus, J., Giorgetta, M., Reick, Ch, Legutke, S., Brovkin, V., Crueger, T., Esch, M., Fieg, K., Fischer, N., Glushak, K., Gayler, V., Haak, H., Hollweg, H.-D., Kinne, S., Kornblueh, L., Matei, D., Mauritsen, T., Mikolajewicz, U., Müller, W., Notz, D., Pohlmann, T., Raddatz, T., Rast, S., Roeckner, E., Salzmann, M., Schmidt, H., Schnur, R., Segschneider, J., Six, K., Stockhause, M., Wegner, J., Widmann, H., Wieners, K.-H., Claussen, M., Marotzke, J., Stevens, B., 2012b. CMIP5 Simulations of the Max Planck Institute for Meteorology (MPI-M) Based on the MPI-ESM-P Model: the MidHolocene Experiment. served by ESGF. WDCC at DKRZ. https://doi.org/10.1594/WDCC/CMIP5.MXEPmh.

Kageyama, M., Braconnot, P., Bopp, L., Mariotti, V., Roy, T., Woillez, M.-N., Caubel, A., Foujols, M.-A., Guilyardi, E., Khodri, M., Lloyd, J., Lombard, F., Marti, O., 2013. Mid-Holocene and Last Glacial Maximum climate simulations with the IPSL model. Part II: model-data comparisons. Clim. Dyn 40, 2469–2495.

Kim, S.-J., Crowley, T.J., Erickson, D.J., Govindasamy, B., Duffy, P.B., Yong Lee, B., 2008. High-resolution climate simulation of the last glacial maximum. Clim. Dyn 31, 1–16.

Lamy, F., Hebbeln, D., Wefer, G., 1999. High-resolution marine record of climatic change in mid-latitude Chile during the last 28,000 years based on terrigenous sediment parameters. Quat. Res. 51, 83–93.

Maldonado, A., Betancourt, J.L., Latorre, C., Villagrán, C., 2005. Pollen analyses from a 50,000-yr rodent midden series in the southern Atacama Desert (25° 30'S). J. Quat. Sci 20 (5), 493–507.

Melo, M., Marengo, J., 2008. The influence of changes in orbital parameters over South American climate using the CPTEC AGCM: simulation of climate during the mid-Holocene. Holocene 18, 501–516.

Otto-Bliesner, B., Brady, E., Clauzet, G., Tomas, R., Levis, S., Kothavala, Z., 2006. Last glacial maximum and Holocene climate in CCSM3. J. Clim. 19, 2526–2544.

Paduano, G.M., Bush, M.B., Baker, P.A., Fritz, S.C., Seltzer, G.O., 2003. A vegetation and fire history of lake Titicaca since the last glacial maximum. Palaeogeogr. Palaeoclimatol. Palaeoecol. 194, 259–279.

Ponce, F., Rabassa, J., Coronato, A., Borromei, A., 2011. Paleogeographic evolution of the Atlantic coast of Pampa and Patagonia since the last glacial maximum to the middle Holocene. Biol. J. Linn. Soc. 103, 363–379.

Prado, L.F., Wainer, I., Chiessi, C.M., 2013a. Mid-holocene PMIP3/CMIP5 model results: intercomparison for the south American monsoon system. Holocene 23 (12), 1915–1920.

Prado, L.F., Wainer, I., Chiessi, C.M., Ledru, M.-P., Turcq, B., 2013b. A mid-Holocene climate reconstruction for eastern South America. Clim. Past 9, 2117–2133.

Rasmussen, K.L., Chaplin, M.M., Zuluaga, M.D., Houze Jr., R.A., 2016. Contribution of extreme convective storms to rainfall in south America. J. Hydrometeorol. 17 (1), 353–367.

Rojas, M., Moreno, P.I., Kageyama, M., Crucifix, M., Hewitt, Ch, Abe-Ouchi, A., Ohgaito, R., Brady, E.C., Hope, P., 2009. The Southern Westerlies during the last glacial maximum in PMIP2 simulations. Clim. Dyn 32, 525–548.

Rojas, M., Moreno, P.I., 2011. Atmospheric circulation changes and neoglacial conditions in the Southern Hemisphere mid-latitudes: insights from PMIP2 simulations at 6 kyr. Clim. Dyn 37, 357–375.

Rostami, K., Peltier, W.R., Mangini, A., 2000. Quaternary marine terraces, sea-level changes and uplift history of Patagonia, Argentina: comparisons with predictions of the ICE-4 G(VM2) model of the global process of glacial isostatic adjustment. Quat. Sci. Rev. 19, 1495–1525.

Taylor, K., Stouffer, R., Meehl, G., 2012. An overview of CMIP5 and the experiment design. Bull. Am. Meteor. Soc. 93, 485–498.

Valero-Garcés, B.L., Jenny, B., Rondanelli, M., Delgado-Huertas, A., Burns, S.J., Veit, H., Moreno, A., 2005. Palaeohydrology of Laguna de Tagua Tagua (34° 30′ S) and moisture fluctuations in Central Chile for the last 46 000 yr. J. Quat. Sci. 20, 625–641.

Voldoire, A., Sanchez-Gomez, E., Salas y Mélia, D., Decharme, B., Cassou, C., Senési, S., Valcke, S., Beau, I., Alias, A., Chevallier, M., Dequé, M., Deshayes, J., Douville, H., Fernandez, E., Madec, G., Maisonnave, E., Moine, M.-P., Planton, S., Saint-Martin, D., Szopa, S., Tyteca, S., Alkama, R., Belamari, S., Braun, A., Coquart, L., Chauvin, F., 2012. The CNRM-CM5.1 global climate model: description and basic evaluation. Clim. Dyn 40, 2091–2121.

Wainer, I., Clauzet, G., Ledru, M.-P., Brady, E., Otto-Bliesner, B., 2005. Last glacial maximum in south America: paleoclimate proxies and model results. Geophys. Res. Lett. 32, L08702. https://doi.org/10.1029/2004GL021244.

Wang, X., Auler, A.S., Edwards, R.L., Cheng, H., Ito, E., Wang, Y., Kong, X., Solheid, M., 2007. Millennial-scale precipitation changes in southern Brazil over the past 90,000 years. Geophys. Res. Lett. 34, L23701. https://doi.org/10.1029/2007GL031149.

Whitney, B.S., Mayle, F.E., Punyasena, S.W., Fitzpatrick, K.A., Burn, M.J., Guillen, R., Chavez, E., Mann, D., Pennington, R.T., Metcalfe, S.E., 2011. A 45 kyr palaeoclimate record from the lowland interior of tropical South America. Palaeogeogr. Palaeoclimat. Palaeoecol 307, 177–192.

Wilks, D.S., 2006. Statistical Methods in the Atmospheric Sciences, second ed. International Geophysics Series. Elsevier Academic Press, St. Louis.

Yukimoto, S., Adachi, Y., Hosaka, M., Sakami, T., Yoshimura, H., Hirabara, M., Tanaka, T.Y., Shindo, E., Tsujino, H., Deushi, M., Mizuta, R., Yabu, S., Obata, A., Nakano, H., Koshiro, T., Ose, T., Kitoh, A., 2012. A new global climate model of the meteorological research institute: MRI-CGCM3-model description and basic performance. J. Meteorol. Soc. Jpn. 90A, 23–64.

Zolitschka, B., Anselmetti, F., Ariztegui, D., Corbella, H., Francus, P., Lücke, A., Maidana, N.I., Ohlendorf, C., Schäbitz, F., Wastegård, S., 2013. Environment and climate of the last 51,000 years - new insights from the Potrok Aike maar lake sediment archive drilling project (PASADO). Quat. Sci. Rev. 71, 1–12.